

# Corrosion of steels with surface treatment and Al-alloying by GESA exposed in lead–bismuth

Annette Heinzl<sup>a</sup>, Masatoshi Kondo<sup>b</sup>, Minoru Takahashi<sup>c,\*</sup>

<sup>a</sup> *Forschungszentrum Karlsruhe, Institut fuer Hochleistungsimpuls-und Mikrowellentechnik, Herrmann von Helmholtz Platz 1, 76344 Eggenstein-Leopoldshafen, Germany*

<sup>b</sup> *Department of Nuclear Engineering, Tokyo Institute of Technology, N1-18, 2-12-1 O-okayama, Meguro-ku, Tokyo 152-8550, Japan*

<sup>c</sup> *Research Laboratory for Nuclear Reactors, Tokyo Institute of Technology, N1-18, 2-12-1 O-okayama, Meguro-ku, Tokyo 152-8550, Japan*

Received 9 June 2005; accepted 12 January 2006

## Abstract

Corrosion tests were performed for T91, E911 and ODS (oxide dispersion strengthened) with surface treatment and Al-alloying by pulsed electron beam (GESA—GepulsteElektronenStrahlAnlage) in flowing lead bismuth eutectic (LBE) with an oxygen content of  $10^{-6}$  wt% at 550 °C for 2000 h. The result was that the surface treatment by GESA led to a faster growing multiphase oxide layer which was very homogenous in thickness. After exposure of specimens to LBE, the average oxide layer at the surface was 14–15  $\mu\text{m}$  thick for ODS, 19–20  $\mu\text{m}$  for E911 and 8–22  $\mu\text{m}$  for T91. No dissolution attack occurred. On the surface of the Al-alloyed specimens, thin protective alumina layers were observed at the places where FeAl was formed by the GESA process, otherwise multiphase oxide layers or corrosion attack were observed.

© 2006 Elsevier B.V. All rights reserved.

PACS: 81.65.Kn; 28.41.Qb; 28.50.Ft

## 1. Introduction

Lead bismuth eutectic (LBE) has been proposed as a candidate for coolant and/or as spallation target material of an accelerator driven subcritical reactor systems (ADS) [1]. One of the critical issues in the design of these systems is the compatibility of steels with LBE. It is known that the formation of an oxide scale on a steel surface can protect it disso-

lution attack by liquid LBE. To stabilize such scales a controlled concentration of dissolved oxygen in LBE has to be maintained. The oxide scale acts as a diffusion barrier for cations and hinders their transport from the steel into the LBE and vice versa [2]. In addition, such an oxide layer must exhibit a low diffusion rate of anions to prevent the steel not only from dissolution but also from strong oxidation. A good bonding to the substrate and matched mechanical and thermal properties are necessary. The properties of the oxide layer could be improved by alloying strong oxide formers like Al or Si into the steel surface. Recent publications

\* Corresponding author. Tel.: +81 3 5734 2957; fax: +81 3 5734 2959.

E-mail address: [mtakahas@nr.titech.ac.jp](mailto:mtakahas@nr.titech.ac.jp) (M. Takahashi).

on corrosion of ferritic–martensitic and austenitic steels with and without Al-coatings or Al additions give an overview on the corrosion effects and processes and their prevention in stagnant and flowing LBE [3–19]. However, few data were presented so far on corrosion behaviour of steels with modified surface structure in LBE.

In this paper, the corrosion behaviour of two ferritic–martensitic steels T91, E911 and a cold-rolled ‘European’ oxide dispersed strengthened martensitic type steel (ODS) are presented. The surfaces of all three steels are modified applying a pulsed electron beam (GESA) with and without alloying of Al into it. The modification without alloying of Al results in structural changes like reduction of grain sizes. Alloying of Al into the surface changes the chemical composition in addition to the structural changes. The corrosion experiments were carried out in flowing LBE with an oxygen concentration of  $10^{-6}$  wt% at 550 °C for 2000 h. The flow velocity in the test section was 1 m/s. After the test, each specimen was investigated based on metallographic analyses.

## 2. Experimental

### 2.1. Loop experiment

The corrosion tests were carried out at a non-isothermal forced lead-bismuth loops at Tokyo Institute of Technology [20]. The loop consists of a main heater, a cooler, a hot and a cold section (high and low temperature region), an electromagnetic pump (EMP), an electromagnetic flow meter (EMF), an oxygen sensor and an expansion and dump tank (Fig. 1). The inventory of liquid Pb/Bi in the loop is about 22 L. The specimens are placed in the test section located in the high temperature region at a temperature of 550 °C. The test section is made of a 9Cr–1Mo steel, STABA 26. An electrical heater, which is positioned just in front of the hot test section maintains the temperature at the desired value. A cooler manufactured of SS316 is placed directly in front of the cold test section. The oxygen activity corresponding to  $10^{-6}$  wt% oxygen in the liquid Pb/Bi is measured by an electrochemical cell (oxygen sensor).

Before LBE was poured in, the loop was heated and filled with high purity argon to clean the inner walls. The LBE was melted in the dump tank at 180 °C and stored for several days. Then the liquid metal was pumped into the loop which was pre-

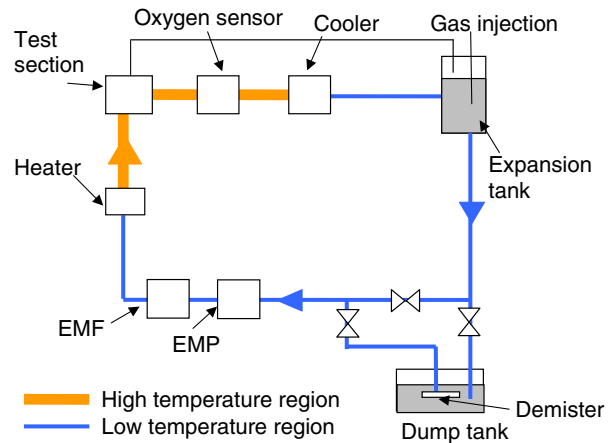


Fig. 1. Diagram of LBE corrosion test loop.

heated to 250 °C. When the LBE flow velocity approached the designated value of 1 m/s, the temperature of the loop was increased to the operation temperature of 400 °C. The electrical heater was used to heat up the test section to 550 °C.

Fig. 2 shows a scheme of the test section. The test specimens with a size of  $15 \times 15 \times 2$  mm<sup>3</sup> were mounted in a cylindrical Mo holder, which was inserted in the test section of the corrosion loop.

### 2.2. Metallographic examinations

After exposure the specimens were washed in hot glycerin at 180 °C to remove the residual LBE. Afterwards the glycerin was removed using water at 80 °C. The cross sections of the samples were examined using light-optical microscope (LOM) and scanning electron microscope (SEM) and applying energy dispersed X-ray analysis (EDX).

### 2.3. Materials

Two ferritic–martensitic steels, T91 and E911, and an ODS all three with surface treatment and surface Al-alloying applying the GESA I facility are tested. The chemical composition of the steels is listed in Table 1.

GESA I is a pulsed electron beam facility which can melt surfaces of steels up to a depth of 40 μm [21]. It consists of a high voltage Marx-generator with a pulse duration control unit (PDCU), a control unit, focusing magnetic coils (MC), a treatment chamber and an electron injector. The latter consists of a multipoint explosive emission cathode (cathode), a controlling grid (grid) and an anode forming

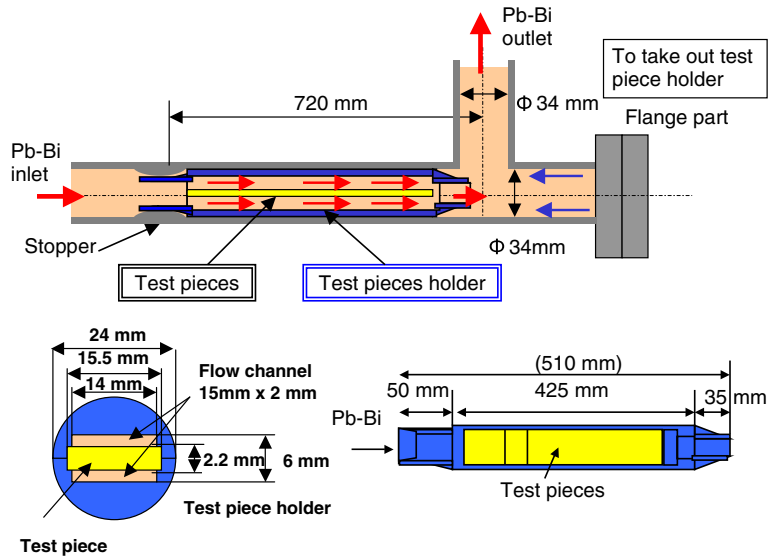


Fig. 2. Test section.

Table 1  
Chemical composition of test steels

wt%	Cr	Ni	Mo	Mn	V	Nb	W	Si	C	Al	N	P	S	Y
ODS	9.28			0.47	0.2			0.62			—	—		0.16
T91	8.26	0.13	0.95	0.38	0.2	0.075	—	0.43	0.1	0.04	0.03	0.02	0.01	
EP911	9.16	0.23	1	0.35	0.23	0.07	1	0.2	0.1	0.007	0.07	0.007	0.003	

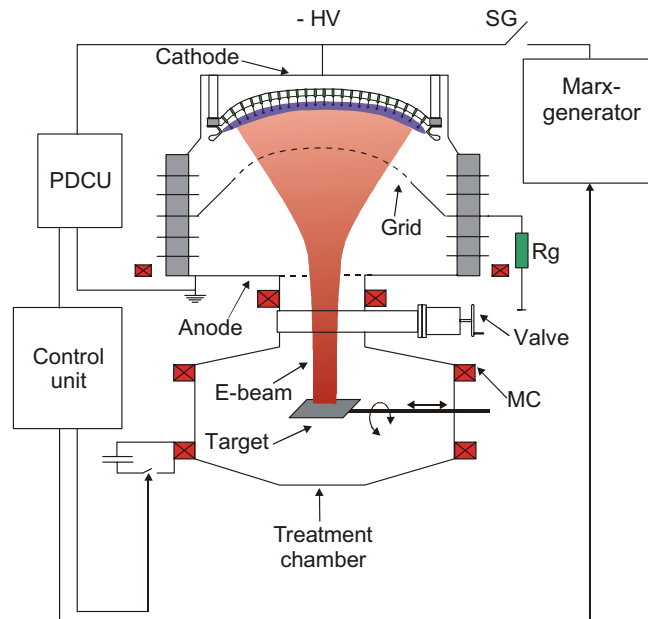


Fig. 3. GESA I test facility.

a triode arrangement. A scheme of the GESA facility is shown in Fig. 3 and its beam parameters are listed

in Table 2. All important parameters for the treatment process like electron energy, power density

Table 2  
Electron beam parameter of GESA I

Electron energy	50–150 keV
Power density	< 2 MW/cm <sup>2</sup>
Pulse duration controllable	2–50 μs
Beam diameter	6–10 cm

and pulse duration can be chosen independent of each other. The electrons are absorbed volumetrically in the target and lead to a rapid melting in the time of several μs. Due to the high cooling rate in the order of 10<sup>7</sup> K/s, fine grained structures develop during solidification of the molten surface layer.

For Al surface-alloying an 18 μm-thick Al-foil was placed on the steel surface. Applying a GESA treatment the Al-foil melts and mixes together with the molten steel surface [22]. A great part of the Al is evaporated during the process, but the remainder, about 25%, is alloyed into the steel [23].

Fig. 4 shows the cross section of ODS after GESA treatment and E911 after Al surface-alloying with the GESA-facility. The etched cross section of the ODS specimen (upper picture) shows a very fine grained structure (< 4 μm) with some coarser grains slightly elongated due to the cold-rolling in the bulk. The restructured surface layer shows grains oriented perpendicular to the surface as a result of the fast cooling process. The structure of E911 (lower picture) is comparable to the one of T91 showing a typical martensitic structure. The mean grain size is about 10–15 μm. After Al surface-alloying by GESA a surface layer of about 20 μm thickness is formed on all steels. The whirling like structure in the restructured layers indicates the turbulent mixing of the Al and the molten steel layer.

### 3. Results

All three steel specimens with just surface treatment show a similar behaviour. After the exposure in LBE their surface is covered with a continuous oxide layer of homogenous thickness exhibiting the typical layered structure (Figs. 5 and 6). The outer layer consists of a porous magnetite layer (Fe<sub>3</sub>O<sub>4</sub>) that breaks off frequently. The rests of the magnetite layer can be observed only at some places (Fig. 5). The inner part of the oxide scale the Fe–Cr–O layer (spinel) sticks on the base material and protects it from liquid metal corrosion. No dissolution attack and no precipitation of LBE into the spinel layer are detected. The ferritic–martensitic steels

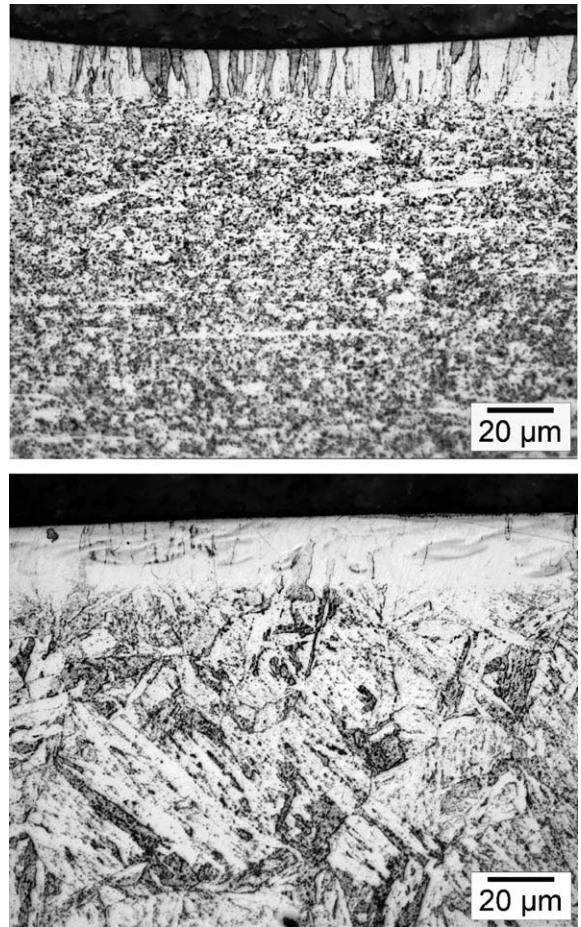


Fig. 4. LOM of cross section. Above: surface treated ODS steel with 20 μm thick restructured surface layer, below: surface alloyed E911 with 20 μm thick restructured surface layer.

show a dense spinel layer with cracks and small disruption at some parts. The cracks run parallel to the surface and stay always within the spinel layer (Fig. 6 below). A pore belt mostly filled with Cr-oxide develops underneath the spinel layer. This is different from the result of the ODS steel. The spinel layer of the ODS has nearly no cracks and does not show any pores underneath (Fig. 6 above). Internal oxidation is rarely detected in case of ODS and E911, while it is more pronounced at the T91. The thickness of the oxide layer without magnetite is about 14–15 μm for ODS, 19–20 μm for E911 and 19 μm for T91. If an internal oxidation zone exists at the T91, the total oxide layer increases to 22 μm.

The specimens with Al-alloying show three different behaviours. The steel was protected by a thin alumina layer on parts with Al concentrations sufficient to form selective Al<sub>2</sub>O<sub>3</sub> oxide scales (Fig. 7). A

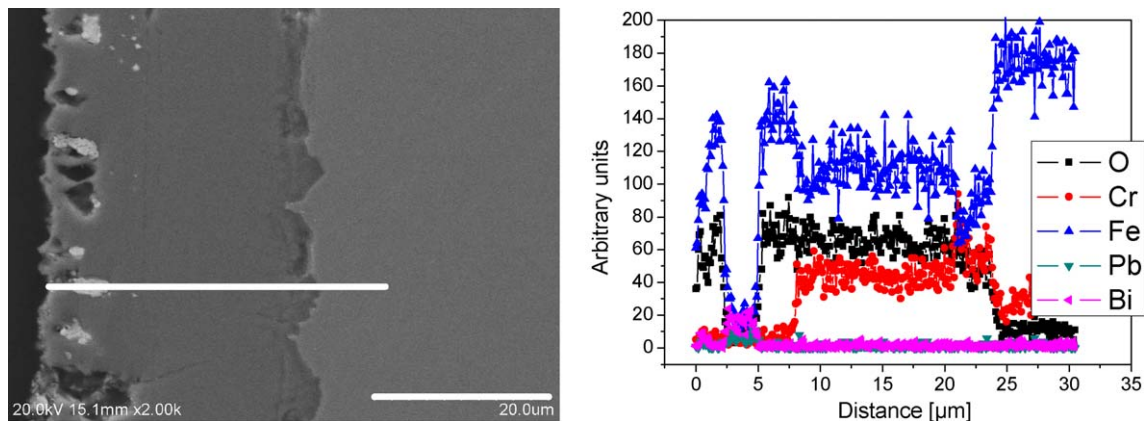


Fig. 5. Left: SEM of cross section of surface treated E911 after 2000 h of exposure to flowing LBE at 550 °C. Right: linescans of elements. Outer layer consists of a Fe and O (magnetite layer), pores are filled with LBE, underneath is a Fe–Cr Spinel.

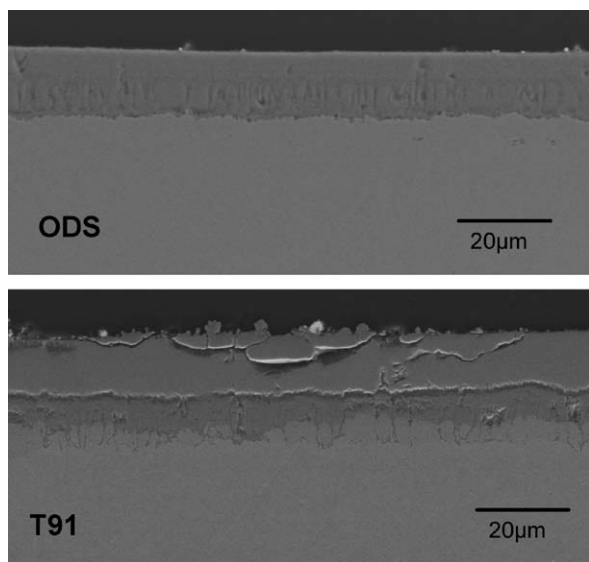


Fig. 6. SEM of cross section of surface treated ODS and T91 after 2000 h of exposure to flowing LBE at 550 °C. A homogeneous oxide layer could be seen with cracks (below).

spinel layer and/or an internal oxidation zone could be observed at parts with an Al concentration lower than required (Fig. 8). Here, the spinel consists of Cr–Fe–Al–O. Wherever the Al concentration was higher than 25 wt%, dissolution of Al is likely and the steels are attacked by LBE (Fig. 9).

#### 4. Discussion

Multi-layered oxide scales are formed on the surface of the ferritic–martensitic steels treated by GESA. The oxide layer protects the steels against dissolution attack. The oxide scale consists of a mag-

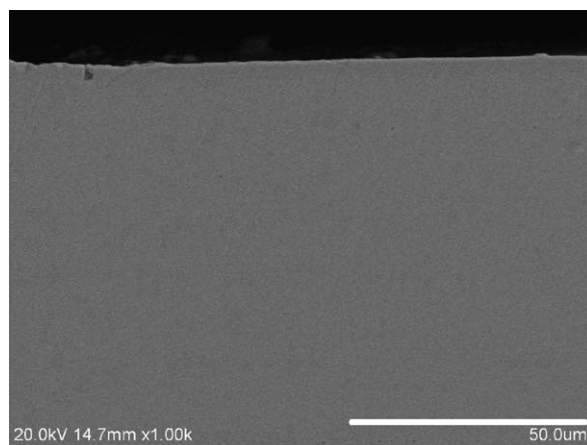


Fig. 7. SEM of cross section of surface alloyed ODS after 2000 h of exposure to flowing LBE at 550 °C showing protective alumina layer at the top.

netite and spinel layer and in case of T91 additionally of an internal oxidation zone. These results are in good agreement with those obtained with the untreated steels [6,7,10,14,19]. Gnocco et al. [14] determined the behaviour of T91 at 550 °C in oxygen saturated, stagnant LBE. After 2000 h exposure the steel was covered with a 7–12 μm thick multiphase oxide layer. Barbier et al. [6,7] found a 14 μm thick oxide scale (including magnetite) at 470 °C under flowing conditions with the same duration oxygen concentration of  $10^{-6}$  wt%. In comparison the thickness of the spinel layer only on the GESA treated T91 reaches 19 μm. This increase in thickness is due to the smaller grain sizes of the modified surface layer. The smaller the grain sizes are, the higher the number of grain boundaries. This leads to higher diffusion rates resulting in an increased oxidation rate,

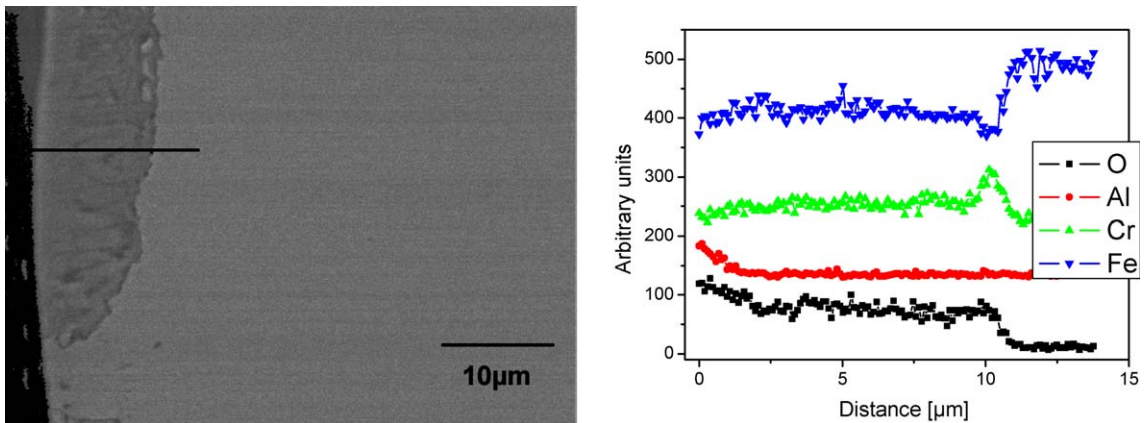


Fig. 8. Left: SEM of cross section of surface alloyed ODS after 2000 h of exposure to flowing LBE at 550 °C with a low Al content at the surface. Right: linescan of elements show a Fe–Cr–Al spinel at the surface underneath a Fe–Cr spinel.

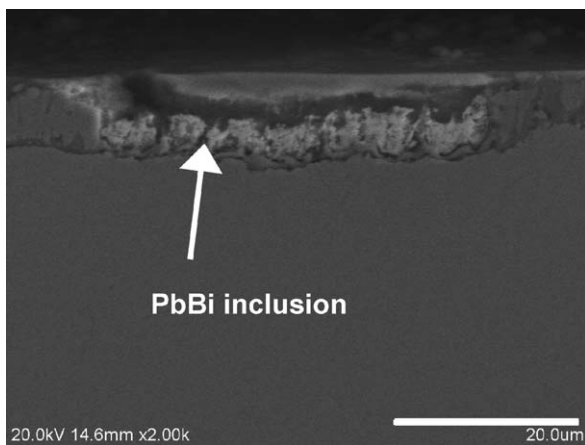


Fig. 9. SEM of cross section of surface alloyed ODS after 2000 h of exposure to flowing LBE at 550 °C with a high Al content at the surface, dissolution attack and PbBi inclusions.

especially at the beginning. The influence of the smaller grain sizes after GESA treatment is also reported for austenitic steel [24]. Although austenitic steels in original state do not develop thick oxide scales in general after exposure in Pb at 550 °C, thick multi-layered oxide scales like on martensitic steels are formed after GESA treatment of their surface.

The three different behaviours that could be observed are in agreement with the results reported in the literature [5,16]. Either dissolution, selective oxidation or normal steel oxidation takes place depending on the Al concentration. If the concentration and therefore the activity of Al in the steel surface is too high, dissolution of Al is very likely and LBE will attack the steel. At low Al concentration, no selective oxidation is possible and the normal multi-layered oxides will grow. FeAl [5]

and/or  $\text{FeAl}_2$  and  $\text{AlCr}_2$  [16] are formed only in case, when the Al concentration ranges between 8 wt% and 25 wt%. Selective growth of thin protective  $\text{Al}_2\text{O}_3$  scales occurs under these conditions. The inhomogeneous Al allocation is a result of the way how the Al-foil was placed on top of the steel. The foil was put by hand on to the steel without any further fixing. A more homogenous distribution will be reachable if an Al coating is used instead.

## 5. Conclusion

Surface treatment by pulsed electron beam leads to a fine grained structure in the treated area influencing the oxidation behaviour. Oxide layers grow quicker on surface treated ferritic–martensitic steels than on untreated steels in LBE. This could be of advantage at lower oxygen concentrations and temperatures but in the case of  $10^{-6}$  wt% rather thick oxide layers are formed. Long-term tests have to be performed to investigate whether these faster growing oxide layers will protect the steel better than oxide layers formed on untreated steels. Especially the long-term stability of oxide scales formed on GESA treated surfaces has to be investigated.

Corrosion tests with surface Al-alloying showed clearly that controlling the Al content is very important to form protective thin oxide layer.

## Acknowledgement

The work has been performed in frame of a JSPS Postdoctoral Fellowship at the Research Laboratory for Nuclear Reactors, Tokyo Institute of Technology.

## References

- [1] C. Rubbia, J.A. Rubio, S. Buono, F. Carminati, Conceptual Design of a Fast Neutron Operated High Power Energy Amplifier, CERN/AT/95-44 (ET), September 29, 1995.
- [2] B.F. Gromov, Y.I. Orlov, P.N. Martynov, K.D. Ivanov, V.A. Gulevski, in: H.U. Borgstedt, G. Frees (Eds.), *Liquid Metal Systems*, Plenum, 1995, p. 339.
- [3] G. Mueller, G. Schumacher, F. Zimmermann, J. Nucl. Mater. 278 (2000) 85.
- [4] G. Benamati, P. Buttol, V. Imbeni, C. Martini, G. Palombardini, J. Nucl. Mater. 278 (2000) 308.
- [5] G. Mueller, A. Heinzl, J. Konys, G. Schumacher, A. Weisenburger, F. Zimmermann, V. Engelko, A. Rusanov, V. Markov, J. Nucl. Mater. 301 (2002) 40.
- [6] F. Barbier, A. Rusanov, J. Nucl. Mater. 296 (2001) 231.
- [7] F. Barbier, G. Benamati, C. Fazio, A. Rusanov, J. Nucl. Mater. 295 (2001) 149.
- [8] G. Benamati, C. Fazio, H. Piankova, A. Rusanov, J. Nucl. Mater. 301 (2002) 23.
- [9] F.J. Martin, S. Soler, F. Hernandez, D. Gomez-Briceno, J. Nucl. Mater. 335 (2004) 194.
- [10] A. Aillo, M. Azzati, G. Benamati, A. Gessi, B. Long, G. Scaddozzo, J. Nucl. Mater. 335 (2004) 169.
- [11] L. Soler, F.J. Martin, F. Hernandez, G. Gomez-Briceno, J. Nucl. Mater. 335 (2004) 174.
- [12] G. Mueller, A. Heinzl, J. Konys, G. Schumacher, A. Weisenburger, F. Zimmermann, V. Engelko, A. Rusanov, V. Markov, J. Nucl. Mater. 335 (2004) 163.
- [13] Ph. Deloffre, F. Balbaud-Célérier, A. Terlan, J. Nucl. Mater. 335 (2004) 180.
- [14] F. Gnocco, E. Ricci, C. Bottino, A. Passerone, J. Nucl. Mater. 335 (2004) 185.
- [15] T. Furukawa, G. Müller, G. Schumacher, A. Weisenburger, A. Heinzl, K. Aoto, J. Nucl. Mater. 335 (2004) 189.
- [16] Y. Kurata, M. Futakawa, S. Saito, J. Nucl. Mater. 335 (2004) 501.
- [17] J. Zhang, N. Li, Y. Chen, A.E. Rusanov, J. Nucl. Mater. 336 (2005) 1.
- [18] K. Schroer, Z. Voss, O. Wedemeyer, J. Novotny, J. Konys, A. Heinzl, A. Weisenburger, G. Mueller, T. Furukawa, K. Aoto, JNC TY9400 2004-023, May 2004.
- [19] M. Mueller, G. Schumacher, A. Weisenburger, A. Heinzl, F. Zimmermann, T. Furukawa, K. Aoto, JNC TY9400 2003-026, January 2004.
- [20] M. Takahashi, M. Kotaka, T. Takahashi, N. Sawada, T. Yano, K. Hata, H. Sekimoto, S. Uchida, T. Suzuki, in: *Proceedings of the 8th International Conference on Nuclear Engineering (INCONE-8)*, Baltimore, MD, USA, April 2–6, 2000, ASME, Paper 8507.
- [21] V. Engelko, B. Yatsenko, G. Müller, H. Bluhm, Vacuum 62 (2001) 211.
- [22] G. Müller, V. Engelko, A. Weisenburger, A. Heinzl, Vacuum 77 (2005) 469.
- [23] G. Mueller, *Korrosionsverhalten von Stählen in flüssigem Blei nach Behandlung mit hochenergetischen gepulsten Elektronenstrahlen*, Dissertation, February 2000, Univ. Karlsruhe.
- [24] H. Glasbrenner, J. Konys, G. Mueller, A. Rusanov, J. Nucl. Mater. 296 (2001) 237.